Semiconductor Physics, Quantum Electronics & Optoelectronics. 2002. V. 5, N 1. P. 101-105.

PACS: 68.49.S, 82.80.M, 61.72.T, V, W, 73.20.H, 68.37.P, 61.43.F

Borophosphosilicate glass component analysis using secondary neutral mass spectrometry

O. Oberemok, P. Lytvyn
Institute of Semiconductor Physics, NAS of Ukraine, 45 prospekt Nauky, 03028 Kyiv, Ukraine
Phone: +380 (44) 265 5940; e-mail: plyt@isp.kiev.ua, obez@isp.kiev.ua

Abstract. In the present study the SNMS technique for the quantitative component analysis of the borophosphosilicate glass layers was used. These layers were deposited on the silicon substrate by chemical vapor deposition method. The charge-up of the surface is compensated by plasma gas electrons in the high frequency mode sputtering. It is shown that modes of such sputtering significantly influence on the macro- and microrelief of the crater during the process of the depth component distribution analysis. An on-off time ratio change of the voltage applied to the sample results in changing the crater shape. At the same time the increase of the sputtering frequency results in appearance of thin protrusions at the crater bottom. Improvement of the depth resolution requires optimization both on-off time ratio and frequency of voltage applied to the sample.

Keywords: borophosphosilicate glass, secondary neutral mass spectrometry, atomic force microscopy, crater shape, roughness, depth profile, depth resolution.

Paper received 31.01.02; revised manuscript received 14.02.02; accepted for publication 05.03.02.

1. Introduction

Borophosphosilicate glass (BPSG) is an important component of the silicon-based semiconductor technology. BPSG have been used as interlevel dielectric films for planarization and passivation of device surfaces. An essential feature of the BPSG layers is reflow [1,2,3] for at relatively low temperatures and small flow angles. As it is shown in [4], the B_2O_3 and P_2O_5 presence increase the thermal expansion coefficient of SiO_2, reducing the stress caused by thermal mismatch with the Si substrate. Layer properties depend on its composition. The phosphorus concentration defines the glass reflow temperature [5]. The boron concentration limits the overmuch reflow providing the better surface planarization. There exists an optimum phosphorus concentration for any given boron concentration to achieve the lowest possible reflow, the minimum flow angles, and hence to obtain the best gap-filling glass. Advanced technology of ultra shallow junctions demands the process temperature to decrease for the dopant diffusion suppression. The optimal temperature range for the advanced technology processes are 700÷900°C. It is this range that used to provide the high reflow level of the BPSG layers. For the BPSG quantitative analysis some methods, such as SIMS- [6,7], XRF- [8], IR- [9,10] spectroscopies are used.

SIMS analysis of the BPSG layers is complicated by charge-up of the sample surface. Sometimes, the charge-up compensation is reached by the electron beam processing or by the metal layer deposition on the surface. In the last case, it is impossible to perform the thick dielectric layer analysis. Besides, the crater effect is the significant problem of the sputtering. The non-rectangular crater shape results in the depth resolution decreasing.

© 2002, Institute of Semiconductor Physics, National Academy of Sciences of Ukraine

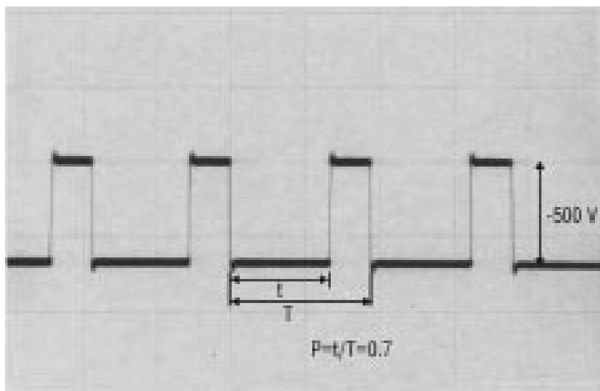

a)

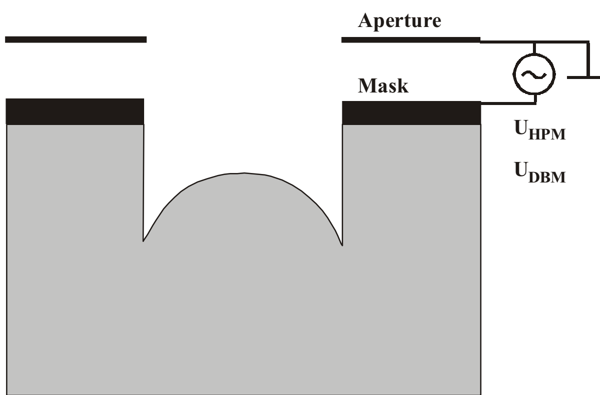

b)

Fig. 1. Voltage shape applied to the sample (a) and schematic crater shape of the dielectric films in the DBM mode and at non-optimal p value in the HFM mode.

The dielectric layer analysis demands the elimination of disadvantages referred above. The SNMS method with high frequency mode (HFM) sputtering is more acceptable for this analysis [11]. Since sputtering and ionization processes are separated in SNMS, the dependence of results from the sample composition is smaller than in SIMS, and use of HFM sputtering enables to minimize the crater effect. In the work we have investigated an influence of the HFM sputtering on accuracy of the quantitative depth component analysis of BPSG.

Experimental and results

BPSG layers (1.2μm thick) were deposited on the Si substrate by the CVD technique at 450°C. A dopant depth distribution quantitative analysis was performed by INA3 instrument (Leybold-Heraues, Berlin, Germany). The primary ion beam was formed by applied square-wave voltage (HFM) between plasma wall and the sample. During the negative pulse (U_{HFM}=500 V), Ar^+ ions from low-pressure (3.26×10^{-3} mbar), high-frequency (27 MHz) Ar plasma are accelerated to the sample and sputter it. Plasma electrons neutralize the accumulated positive surface charge while the voltage is absent. HF-generator was used as a high-frequency voltage source with adjustable frequency (f) and on-off time ratio (p) of pulses. The voltage shape applied to sample is shown in Fig. 1a.

The plasma potential and electron-ionization current, measured by the Langmuir probes, are of 3 V and 0.35 mA, respectively. The DEKTAK 3030 (Veeco) profilometer was used for the crater shape and sputtering rate measurements. We investigated the uniformity and structureof the sample surface after 10 min sputtering at different conditions by the atomic force microscopy (AFM). The dopant concentration quantitative analysis on the depth was carried out taking into account relative sensitivity factors (RSF). For RSF determination, the SiO_2/Si structure was implanted by boron and phosphorus. We evaluated RSF's from the expression:

$$\frac{1}{RSF}=\frac{I(Si^0)C_X}{I(X^0)C_{Si}}$$

where $I(Si^0)$ – secondary neutrals intensity for bulk silicon (reference element),

$I(X^0)$ – secondary neutrals intensity for the element X

C_X – X concentration,

C_{Si} – Si concentration

The RSF for oxygen was determinted from its known concentration in the SiO_2 film (2.45×10^{22} at/cm^3). Results of these calculations are shown in Tab.1.

Element	E implant. keV	Dose, cm^{-2}	RSF
P	180	1×10^{16}	0.380
B	50	6×10^{15}	1.012
O	-	-	0.012
Si	-	-	1

The depth resolution was evaluated by the expression:

$$R_F=\Delta Z/Z\times 100\ \%,$$

where ΔZ – difference of depths at the 16 and 84% of signal intensity;

Z – depth at the 50% signal intensity;

F – frequency of sputtering.

1. Crater shape dependence on the sputtering modes

During the dielectric or semiconductor film sputtering in the direct bombardment mode (DBM), the crater shape is essentially non-uniform (Fig. 1b.). The crater shape and sputtering rate depend on the voltage (U_{DBM}) applied to the sample.

The sputtering rate is higher in areas close to the crater edges that are limited by a metal mask.

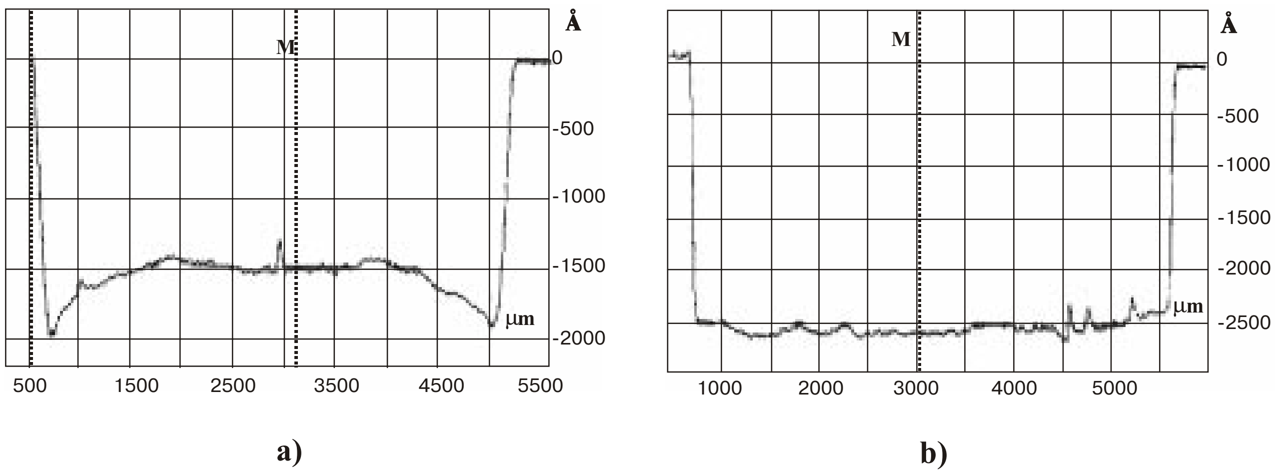

Fig. 2. The crater profiles in the BPSG film after 10 min sputtering at f=50 kHz (a- p=0.5; b- p=0.7).

a)

b)

c)

d)

Fig. 3. Surface micro-relief of the as-deposited BPSG film (a), obtained after 10 min sputtering by SNMS at p=0.5 for f=50 kHz - (b), at p=0.7 for f=50 kHz - (c) and at p=0.7, f=400 kHz - (d).

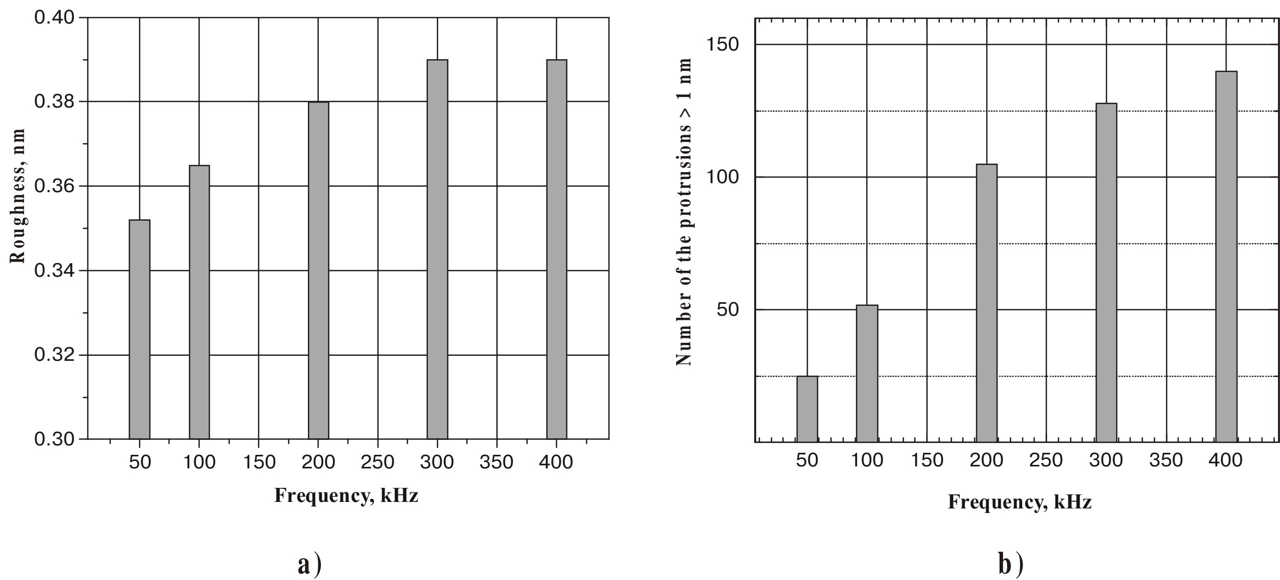

Fig. 4. Frequency dependences of the roughness (a) and number (b) of the protrusions (>1nm).

Moreover, the shape of crater bottom has the hemisphere form. These non-uniformities are connected with the surface charge-up during the sample sputtering. Use of HFM sputtering is one of the possibilities to compensate the surface charge-up [11]. For realization of this mode, high-frequency voltage (U_{HFM}) is applied between the sample mask and the aperture (Fig. 1b). The crater shapes obtained at different p values are shown in Fig. 2. The obtained results show that on-off time ratio essentially influence the crater shape in BPSG layers. Fitting of on-off time ratio of applied voltage is possible to receive the almost rectangular crater shape. Thus at f=50 kHz and p=0.5, the crater shape is more uniform as compared with the DBM mode but has the non-uniform residual pattern (Fig. 2a.).

At p=0.7, the crater shape is close to the rectangular one (Fig. 2b.). At this p value for f=50 kHz (optimal sputtering conditions for BPSG film), increase of the sputtering frequency does not result in essential modifications of the crater shape. It is necessary to note that during the sputtering time, the crater shape is not changed at optimal conditions. Non-optimal conditions lead to the increase of the distance between depths of central and peripheral parts of the crater during sputtering.

2. Surface structure on the crater bottom

Microrelief of as deposited BPSG films is shown in Fig. 3a. The surface has a significant roughness (0.93 nm). The maximal height of protrusions reaches 13.07 nm. After sputtering at f=50 kHz and p=0.5 the roughness is less (0.72 nm) but the maximal height of protrusions increases to 13.88 nm (Fig. 3b). At p increase up to 0.7, surface shape becomes nearly thick and high protrusions at optimal sputtering conditions. The reasons of this phenomenon demand additional investigations.

In Fig. 4, the change of structural properties of the surface on sputtering frequency are shown.

At p=0.7, increase of the sputtering frequency from 50 kHz to 400 kHz results in the surface roughness increase from 0.35 nm to 0.39 nm (Fig. 4a.). Also, it results in the increase of the small protrusion number with the height larger than 1 nm (Fig. 4b.) on the 3μm×3μm area (Fig. 3d.). Thus, sputtering frequency increase leads to the essential micro-relief evolution and, therefore, to decrease of the depth resolution.

3. Dopant distributions in the BPSG/Si structure

Fig. 5 illustrates the BPSG depth profiles for B, P, O, Si measured at f=50 kHz (solid lines) and 400 kHz (dashed lines). Thickness of BPSG layer was 1.2 μm. More overextended tails (dashed lines) of the boron and phosphorus indicates the depth resolution decrease (R_{50}=7.9% and R_{400}=8.6% for phosphorus). Obviously, mechanism of this phenomenon is connected to charge transfer. Some plasma gas electrons have no time to reach the surface sample. Thus, the frequency increase results in the decrease of the charge-up compensation. In this case, ΔR is 0.7%. Estimated element concentrations of B, P, O and Si near the BPSG/Si interface are 24, 12, 30, 34 %, respectively.

Conclusion

In the present study, the analysis of the influ-

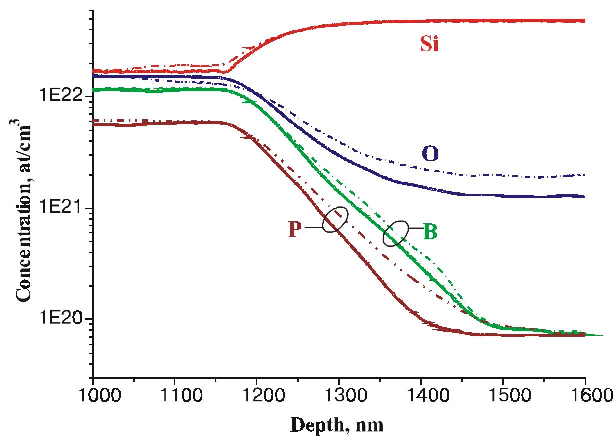

Fig. 5. Dopants distribution in BPSG/Si structure.

ence of HFM sputtering mode on the BPSG micro- and macrorelief was carried out. It is shown that the change of the sputtering voltage on-off time ratio enables to reach the near-rectangular crater shape. But it does not provide the microuniformity of the BPSG sputtering. Increase of the frequency sputtering leads to the evolution of the BPSG microrelief. There is a plenty of fine protrusions higher than 1nm at the bottom of a sputtering surface. Presence of these protrusions results in the depth resolution worsening. The latter is confirmed by the R increase. In order to obtain the high depth resolution and, accordingly, high-quality concentration analysis of BPSG layers, the sputtering parameters (p, f) should have the optimum values. Thus, not only on-off time ratio of applied voltage, but also the frequency influences on accuracy of concentration measurements, which was not specified earlier for INA3 SNMS instrument.

References

1. D.S. Walsh, B.L. Doyle, Simultaneous nuclear reaction analyses of boron and phosphorus in thin borophosphosilicate glass films using (б,p) reactions // *Nuclear Instruments and Methods in Physics Research B* **161-163** pp. 629-634 (2000)
2. A.C. Sharp, J. Patel, Borophosphosilicate glass for VLSI device fabrication // *Vacuum* 35 (10-11), pp. 441-443 (1985)
3. P.J. French, R.F. Wolffenbuttel, Reflow of BPSG for sensor applications // *Journal of Micromechanics and Microengineering* 3 (3), pp. 135-137 (1993)
4. Choon-Gi Choi, Myung-Yung Jeong, Tae-Goo Choy, Characterization of borophosphosilicate glass soot fabricated by flame hydrolysis deposition for silica-on-silicon device applications // *Journal of materials science* 34 pp. 6035- 6040 (1999)
5. W. Kern, G. L. Schnable, Chemically vapor-deposited borophosphosilicate glasses for silicon device applications // *RCA Review* 43 (3), pp. 423-457 (1982).
6. P. K. Chu, S. L. Grube, Quantitative determination of boron and phosphorus in borophosphosilicate glass by secondary ion mass spectrometry // *Analytical Chemistry* 57 (6), pp. 1071-1074 (1985).
7. Leisch, M. Surface analysis of dielectric films by time-of-flight-secondary ion mass spectrometry // *Vacuum* 43 (5-7), pp. 481-483 (1992).
8. N. Perekh, C. Nieuwenhuizen, J. Borstrok and O. Elgersma, Analysis of thin films in the silicon integrated circuit technology by X-ray fluorescence spectrometry // *J.Electrochem. Soc.*, 138 (5), pp. (1991).
9. L. Zhang, J. E. Franke, T. M. Niemczyk, D. M. Haaland, Optimized external IR reflection spectroscopy for quantitative determination of borophosphosilicate glass parameters // *Applied Spectroscopy* 51 (2), pp. 259-264 (1997).
10. T.M Niemczyk, S. Zhang, J. E. Franke, D. M. Haaland, Quantitative determination of borophosphosilicate glass thin-film properties using infrared emission spectroscopy // *Applied Spectroscopy* 53 (7), pp. 822-828 (1999).
11. R. Krimke, H. M. Urbassek and A. Wucher, “High-frequency electron-gas secondary neutral mass spectrometry”, evaluation of transient effects // *J. Phys. D: Appl. Phys.* 30 pp. 1676–1682, (1997).